Nuclear Inst. and Methods in Physics Research, A 916 (2019) 226–229

Contents lists available at ScienceDirect

Nuclear Inst. and Methods in Physics Research, A

journal homepage: www.elsevier.com/locate/nima

Irradiation studies of a multi-doped $Gd_3Al_2Ga_3O_{12}$ scintillator

V. Alenkov [a], O. Buzanov [a], G. Dosovitskiy [b], V. Egorychev [c], A. Fedorov [d], A. Golutvin [e,f], Yu. Guz [g,*], R. Jacobsson [h], M. Korjik [b,d], D. Kozlov [d], V. Mechinsky [d], A. Schopper [h], A. Semennikov [c], P. Shatalov [c], E. Shmanin [e]

[a] FOMOS Crystals, Moscow, Russia
[b] NRC "Kurchatov Institute", Moscow, Russia
[c] Institute for Theoretical and Experimental Physics, NRC "Kurchatov Institute"-ITEP, Moscow, Russia
[d] Institute for Nuclear Problems of Belarus State University, Minsk, Belarus
[e] NUST MISIS, Moscow, Russia
[f] Imperial College London, London, United Kingdom
[g] Institute for High Energy Physics, NRC "Kurchatov Institute"-IHEP, Protvino, Russia
[h] CERN, Geneva, Switzerland

ARTICLE INFO

Keywords:
Electromagnetic calorimetry
Scintillation crystal
Gadolinium-aluminum-gallium garnet
Radiation damage
Optical transmission

ABSTRACT

The characteristics of a $Gd_3Al_2Ga_3O_{12}$ crystal scintillator doped with cerium and co-doped with magnesium and titanium have been studied, mainly in view of using it for the Phase II upgrade of the LHCb electromagnetic calorimeter. Samples of the scintillator were irradiated with γ (^{60}Co) to 2 kGy and with 24 GeV protons to 900 kGy. The proton fluence value was $\sim 3 \cdot 10^{15}$cm^{-2}. It was found that γ-irradiation did not produce any change in the optical transmission of the crystals in the spectral range of the scintillation light, whereas a degradation after the proton irradiation was measurable. For the 1 cm thick sample, a loss of transmission of 3.6% was measured at the wavelength of maximum scintillation (520 nm), and the measured induced absorption coefficient at this wavelength was ~3.6 m^{-1}. The formation of radioisotopes in the crystal at proton irradiation has been analysed. The formation of isotopes was also simulated with the help of the FLUKA package. The simulation was found to be in a good agreement with experimental results. The results have been used to estimate the expected intensity of parasitic radio-luminescence at high-luminosity operation in a GAGG/W sampling electromagnetic calorimeter.

1. Introduction

Scintillators are widely used in both homogeneous and sampling calorimeters of high energy experiments operating at moderate radiation doses. Homogeneous electromagnetic calorimeters using bismuth germanate $Bi_4Ge_3O_{12}$ (BGO) and lead tungstate $PbWO_4$ (PWO) were successfully taking data in the L3, CMS and ALICE experiments at CERN [1,2]. Sampling calorimeters with plastic based scintillators as active medium have also proven very good performance. Most of them use the Shashlik technology with wavelength shifting (WLS) fibres for the light collection [3,4], but designs with direct scintillation light output also exist (e.g., SpaCal technology [5]).

The future physics program at the High-Luminosity LHC will involve significant increase of the integrated luminosity. Consequently very harsh radiation background and high occupancy are expected in the regions close to the beam. For example, after the LHCb Phase II upgrade it is foreseen to operate the detector at a luminosity of up to $2 \cdot 10^{34}$ cm^{-2} s^{-1} and collect up to 300 fb^{-1} of data. At such integrated luminosity, the total ionization dose (TID) collected by the innermost ECAL cells will reach ~1 MGy, with a fluence of charged hadrons of $\sim 10^{15}$ cm^{-2} and neutrons of $\sim 5 \cdot 10^{15}$ cm^{-2} (1 MeV neutron equivalent) [6]. The present LHCb ECAL is a sampling calorimeter (Shashlik) based on plastic scintillator [3]. It is expected to show a significant degradation after collecting a dose of ~20 kGy [7] and to become inoperable after 40–50 kGy. Moreover, the high luminosity leads to high event pile up and high shower density in the central area of the detector. Simulation studies indicate that overlapping showers will affect the calorimeter performance in the LHCb Upgrade conditions.

For this reason, a replacement of the innermost ECAL modules in the LHCb ECAL with sampling calorimeter modules based on radiation-hard dense crystalline scintillators is considered. Using dense scintillators and converters one can build calorimeter with smaller Moliere radius, which will improve the shower separation. The Moliere radius of the present LHCb ECAL is about 36 mm, while, for example, for the tungsten–GAGG sampling calorimeter with volume ratio of 1:1 it is 13 mm.

Another powerful way of improving the LHCb ECAL performance at the High-Luminosity LHC is to add a fast-timing measurement to the

* Corresponding author.
E-mail address: Iouri.Gouz@cern.ch (Y. Guz).

https://doi.org/10.1016/j.nima.2018.11.101
Received 19 June 2018; Received in revised form 19 November 2018; Accepted 19 November 2018
Available online 22 November 2018

Table 1
Scintillation properties of some prospective Ce-doped scintillation materials in comparison with $PbWO_4$ and plastic scintillator.

Scintillator	ρ, g/cm^2	X_0, cm	Light yield ph./MeV	τ_{sc}, ns	λ_{max} nm	Irradiation results
$Y_3Al_5O_{12}$:Ce	4.55	3.28	11 000	70	550	[13]
(Lu-Y)$_2SiO_5$:Ce	7.0	1.2	30 000	35	420	[14]
Lu_2SiO_5:Ce	7.4	1.1	27 000	40	420	[9]
$Gd_3Al_2Ga_3O_{12}$: Ce, Mg, Ti	6.67	1.61	36 000	36(73%) 122(27%)	520	This paper
$PbWO_4$	8.28	0.89	100	6	420	[2]
Polystyrene: PTP, POPOP	1.06	41.3	12 000	3	430	[15]

detector, in order to suppress combinatorial background resulting from multiple interactions. The fast timing requires choosing a scintillator with a large light yield and fast response time. A physics driven optimization [6] is ongoing to decide on the upgraded calorimeter design. A similar optimization work has started for the electromagnetic calorimeter of the recently proposed TauFV experiment at the CERN SPS [8].

All known crystalline self-activated (intrinsic) scintillation materials show considerable degradation of the transparency after hadron irradiation [9]. For example, for PWO crystals a significant damage of the optical transmission was observed after proton irradiation with fluences of $\sim 10^{13}$ p/cm^2 [10,11].

Cerium doped scintillation materials of orthosilicate and garnet structure show better tolerance to all types of irradiation [9]. The (Lu-Y)$_2SiO_5$ (LYSO) scintillator was recently considered for application as active medium in a Shashlik-like design for the upgrade of the CMS Endcap Calorimeters, to be exploited at High-Luminosity LHC [12]. Table 1 summarizes the properties of several commercially available scintillation materials which have been subject to detailed radiation tolerance studies.

It has been found that Ce-doped garnet type crystals are the most tolerant to different types of radiation. As an example, the results of irradiation studies of Ce-doped $Y_3Al_5O_{12}$ (YAG) can be found in [13].

Another Ce-doped garnet type scintillation material, $Gd_3Al_2Ga_3O_{12}$ (GAGG), has the highest light yield among considered orthosilicate and garnet type materials. Co-doping with Mg is used to significantly improve its scintillation decay time and suppress phosphorescence [16]. Co-doping with Ti is used to prevent the stabilization of Ce ions in the tetravalent state [17,18]. GAGG does not contain expensive elements in its composition: Gadolinium is much cheaper than Lutetium, which is beneficial for the construction of large detectors. For the crystals produced at a high temperature by Czochralski method, the raw material contributes about 30% of the scintillator price. The Gadolinium oxide is 5–7 times cheaper than the Lutetium oxide. It can decrease the price by 20%. The temperature of crystallization for GAGG is 200 °C less than for LSO-LYSO, this can further decrease the price by 5%. Thus, at mass production the price of GAGG will be at least 25% lower.

In this article we report on our studies of the scintillation signals and radiation damage effects in multi-doped GAGG scintillation crystals at very high proton fluence, exceeding $3 \cdot 10^{15}$ particles/cm^2. We have found that these crystals have outstanding radiation tolerance and fast scintillation signal, which, together with its high light yield and high density, make them one of the best choices for calorimetry in future High Energy Physics experiments.

2. Samples and measurements

The samples for our tests were supplied by the FOMOS Crystals company (Moscow, Russia). Crystals doped with Ce and co-doped with Mg and Ti were grown by the Czochralski method from an iridium crucible. The ingots were then annealed at 750 °C during 50 h before the production of the samples [17,18]. Samples with lateral dimensions 20 × 20 mm^2 and a thickness of 2 mm and 10 mm were prepared.

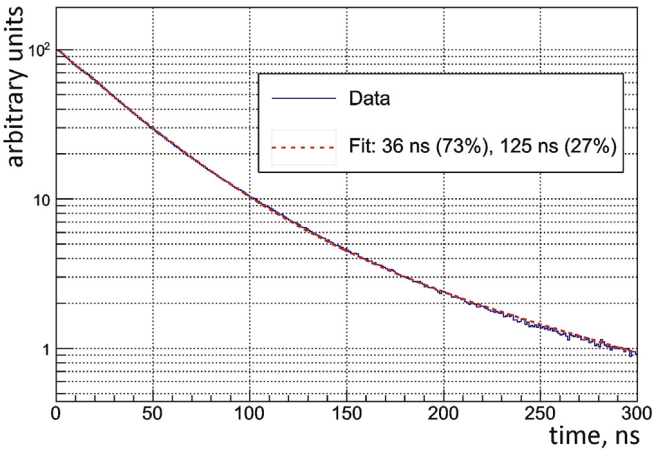

Fig. 1. GAGG:Ce, Mg, Ti scintillation signal shape.

To characterize the radiation damage in the crystals, the optical transmission in the samples was measured before and after irradiation using a Varian Cary 50 spectrophotometer. All measurements were done at room temperature.

To detect possible presence of post-growth defects in the crystal, the samples were irradiated with a ^{60}Co source [9] (1.22 MeV photons, 2000 Gy absorbed dose, dose rate 1000 Gy/h) at the Minsk irradiation facilities. The optical transmission has been measured 30 min after the γ-irradiation. No change with respect to the measurements before irradiation was found.[1]

Another set of samples, cut from the same ingot, was irradiated by 24 GeV/c protons at the CERN Proton Synchrotron (PS) during 10 days up to an accumulated fluence of about $1.3 \cdot 10^{15}$ and $3.1 \cdot 10^{15}$ p/cm^2 for different samples. This corresponds to a TID dose of 370 kGy and 910 kGy in GAGG, respectively. The fluence was measured by Al foil radiation monitors.

Due to the activation of the crystals it was not possible to measure their optical transmission immediately after the irradiation. Measurements of the optical transmission have been done two months later, as soon as the induced radioactivity had fallen to acceptable levels for personnel radiation protection standards. Subsequently, the set of radioisotopes created in the samples have been measured by the CERN Radiation Protection service using an HPGe coaxial BE2830 Canberra detector.

3. Experimental results

Fig. 1 shows the time distribution of scintillation photons from the GAGG:Ce, Mg, Ti measured in the non-irradiated samples using cosmic rays. The signal was read out using a HAMAMATSU R7899-20 PMT and recorded with a LECROY WR8104 oscilloscope. The shape shown in Fig. 1 is an average of 10 000 signals fitted with a sum of two exponentials. The scintillation signal decay time is similar to that obtained for GAGG:Ce, Mg [19].

Fig. 2a shows the optical transmission in a 1 cm thick crystal before and after irradiation. Fig. 2b shows the spectrum of induced absorption $d\kappa$ obtained from the two graphs of Fig. 2a: $d\kappa = 1/s \ln\left(\frac{T_{before}}{T_{after}}\right)$, where s is the sample thickness, T_{before} and T_{after} are the levels of transmission before and after irradiation, respectively. The error bars in Fig. 2b correspond to the transparency measurement precision of 0.2%. It was not possible to determine the induced absorption below 480 nm, as

[1] Results of a γ-irradiation to 120 kGy of GAGG:Ce co-doped with Mg can be found in [19]. No change in the light transmission at the scintillation wavelength was detected in this study.

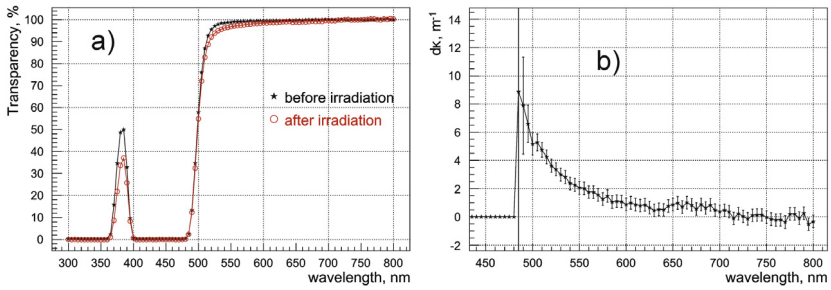

Fig. 2. (a) Optical transmission in a 1 cm thick GAGG crystal before (stars) and after (open circles) irradiation with protons with fluence of $3.1 \cdot 10^{15}$ p/cm^2; (b) irradiation induced absorption coefficient for fluence of $3.1 \cdot 10^{15}$ p/cm^2.

Table 2
List of isotopes measured two months after the irradiation in the 1 cm thick GAGG crystal.

Isotope	A, Bq	Isotope	A, Bq	Isotope	A, Bq
Be-7	7.23E+05	As-74	1.14E+04	Pm-143	1.04E+05
Na-22	1.96E+04	Se-75	3.13E+04	Pm-144	2.50E+04
Sc-46	7.52E+04	Rb-83	6.43E+04	Eu-146	6.96E+04
V-48	4.39E+04	Rb-84	1.73E+04	Gd-146	6.89E+04
Cr-51	1.63E+05	Sr-85	6.84E+04	Eu-147	2.81E+05
Mn-54	4.95E+04	Y-88	3.20E+04	Eu-148	2.34E+05
Co-56	3.54E+04	Zr-88	8.59E+04	Pm-148m	3.54E+04
Co-57	5.54E+04	Ag-105	7.93E+04	Eu-149	4.08E+05
Co-58	1.85E+05	Sn-113	1.35E+05	Gd-149	2.85E+04
Fe-59	3.31E+04	Te-121	9.49E+04	Gd-151	2.75E+05
Co-60	8.51E+03	Xe-127	1.89E+05	Gd-153	2.58E+05
Zn-65	1.88E+05	Ba-131	5.64E+04	Eu-156	1.13E+05
Zn-72	1.55E+04	Ce-139	1.97E+05		

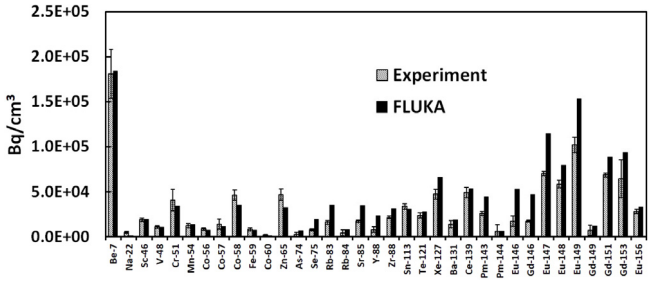

Fig. 3. Comparison of the measured set of isotopes (grey), and their level of activities and the prediction by a FLUKA simulation (black) of the equivalent conditions of irradiation.

the transmission at these wavelengths is close to zero due to a strong absorption by Ce^{3+} ions, both before and after irradiation. As shown in Fig. 2b, above 480 nm, the induced absorption, dk, decreases smoothly with increasing wavelength. This may suggest that the observed absorption curve constitutes the tail of the full absorption band of the colour-centres, with a maximum in the UV range. The absorption induced by proton irradiation has only a very slow spontaneous recovery [9]. This was supported by later measurements of the same samples, three, four and five months after the irradiation. These measurements are compatible within the measurement errors. It is expected that the induced absorption immediately after the irradiation is close to the measured values.

Table 2 shows the list of long-lived isotopes detected in the GAGG crystal after irradiation with protons. Fig. 3 shows a comparison of the measured set of isotopes and their level of activities with the prediction from a simulation of the equivalent conditions of the irradiation with the FLUKA v.2011.2x-0 package [20].

A reasonable agreement is observed between the measurements and the simulated results. Some discrepancy could be partially explained by the attenuation of the photons used for identification in the relatively thick sample. This validates usage of FLUKA simulation for further studies.

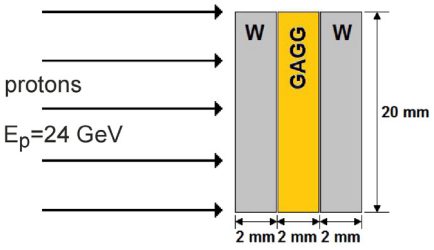

Fig. 4. Sketch of the element of the detecting module used for simulation.

4. Discussion

The good tolerance of the GAGG crystal optical transmission to proton irradiation is confirmed. However the decay of the created radionuclides leads to a parasitic scintillation which produces additional noise for the energy measurement with the calorimeter. It is important to estimate the intensity of this parasitic radio-luminescence caused by the decays of the radioisotopes.

As pointed out above, operating at very high luminosity requires a very dense calorimeter with a small Moliere radius. Together with the requirement of large light yield, it is therefore reasonable to consider the case of a sampling calorimeter with a tungsten converter with equal volumes of GAGG and W, which has radiation length of ~5.7 mm and Moliere radius of ~12.5 mm.

The dose rate caused by the decay of the induced radio-isotopes in the GAGG was studied using a FLUKA simulation. For this study we used a detector element layout consisting of a single slice of a Shashlik type module, illustrated in Fig. 4. The radiation field in the centre of the LHCb calorimeter was emulated by 24 GeV protons. The time profile corresponds to the most aggressive scenario of the upgraded LHCb data taking (Fig. 5); the proton flux was set to $9.7 \cdot 10^7$ particles/cm^2/s, such that the total TID dose for the whole period was 910 kGy. This is close to the dose expected at the centre of the LHCb calorimeter after achieving the planned integrated luminosity of 300 fb^{-1} [6].

Fig. 5 shows time profiles of the proton fluence in one of the possible scenarios, and of the absorbed dose rate in the GAGG plate caused by the decays of the radioisotopes created in the GAGG and tungsten plates.

It turns out that the dose rate increases at the start of the beam operation and decreases at the stop of the beam with a time constant of ~10^4 s, which is the typical decay time for most of the short-lived isotopes. At the stop of the beam the dose rate decreases by a factor of about 100, which means that most of the dose rate is determined by these short-lived isotopes. It also means that at lower luminosity the radio-luminescence dose rate will be proportionally lower.

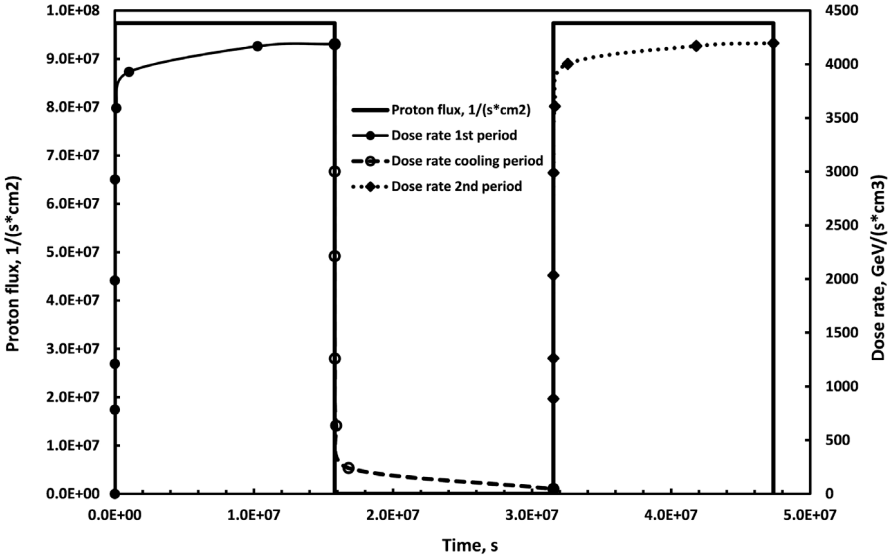

Fig. 5. Time profile of the proton flux and induced absorbed dose rate in a $20 \times 20 \times 2$ mm^3 GAGG scintillation plate.

With these results we can evaluate the corresponding noise from the radio-luminescence and compare it with the signal for the case of the LHCb electromagnetic calorimeter [3]. A detector cell consisting of equal volumes of GAGG scintillator and tungsten converter, having lateral dimensions of 12×12 mm^2 and length of 14 cm (25 radiation lengths), will contain a total of 10 cm^3 of GAGG. The energy deposition in the GAGG from the radio-isotopes in the 25 ns time window, which is the interval between two consecutive bunch crossings at the LHC, can be estimated from Fig. 5. It is of the order of 1 MeV. The "calibration constant", which is the ratio of the total energy deposition in the cell to the energy deposition in the scintillator (visible energy), $E_{dep}^{total}/E_{dep}^{visible}$, for this configuration is estimated to be about 4. Thus, we can conclude that the average energy deposition due to the radio-luminescence in the 25 ns time interval is equivalent to ~4 MeV of reconstructed energy.

The radio-luminescence contribution of 4 MeV has to be compared to the dynamic range of energies of the particles detected in the central region of the LHCb electromagnetic calorimeter. In the present detector [3], the signals are being integrated in 25 ns intervals and digitized with a 12 bit ADC. The detector calibration is such that one ADC count corresponds to 2.5 MeV of photon *transverse* energy, which in the central region of the calorimeter translates to 50–120 MeV of particle energy. Thus the radio-luminescence contribution is much less than one ADC count.

We foresee to conduct more detailed studies in the future, in order to better estimate the magnitude and the fluctuations of the radio-luminescence noise for each specific calorimeter configuration in different experiments.

5. Conclusion

The irradiation studies showed a very good radiation hardness of GAGG:Ce scintillators co-doped with Mg and Ti. The induced absorption coefficient at the wavelength of maximum scintillation, 520 nm, measured after irradiation by 24 GeV protons at the CERN PS to a fluence of $3.1 \cdot 10^{15}$ protons/cm^2 amounts to ~3.6 m^{-1}. Gamma spectroscopy was performed two months after the irradiation. FLUKA simulation agrees reasonably well with the measured results. The level of radio-luminescence caused by decays of the created radioactive isotopes for a possible configuration of the LHCb ECAL was estimated. It was shown that the corresponding noise signal integrated in the 25 ns time window in a detector cell made of $12 \times 12 \times 2$ mm^3 GAGG plates is negligible compared to other contributions.

We can conclude that the multi-doped GAGG scintillator is a good candidate as active medium in the electromagnetic calorimeters to be operated in the harsh radiation environment of the experiments at the High-Luminosity LHC.

Acknowledgements

Authors are greatly indebted to M. Glaser, F. Ravotti and G. Pezzullo for the irradiation of the samples at the IRRAD facility at CERN, and to N. Riggaz for the gamma spectroscopy of the samples after irradiation. Authors also would like to thank Drs. E. Auffray and A. Singovski from the CMS Collaboration (CERN) for fruitful discussions and assistance during the measurements.

This work has received funding from the European Union's Horizon 2020 research and innovation programme under grant agreement No. 654168 and was supported by grant No. 14.W03.31.0004 of the Russian Federation Government.

References

[1] The CERN Large Hadron Collider: Accelerator and Experiments, Vol. 1-2, CERN, Geneva, 2009.
[2] P. Lecoq, A. Gektin, M. Korzhik, Inorganic Scintillators for Detector Systems, Springer, 2017, p. 408.
[3] LHCb Collaboration, The LHCb detector at the LHC, JINST 3 (2008) S08005.
[4] G. David, et al., IEEE Trans. Nucl. Sci 45 (1998) 692–697;
K.H. Ackermann, et al., STAR detector overview, NIM A499 (2003) 624.
[5] R.-D. Appuhn, et. al, The H1 lead/scintillating-fibre calorimeter, NIM A 386 (1997) 397–408.
[6] LHCb Collaboration, Expression of Interest for a Phase-II LHCb Upgrade: Opportunities in avour physics, and beyond, in the HL-LHC era, CERN-LHCC-2017-003.
[7] Yu Guz, et al., JINST 12 (07) (2017) C07024.
[8] G. Wilkinson, et al., TauFV: a fixed-target experiment to search for flavour violation in tau decays, in: Physics Beyond Colliders workshop, CERN, 13-14 June 2018.
[9] E. Auffray, M. Korjik, IEEE Trans. Nucl. Sci. 63 (2) (2016) 552–563.
[10] M. Huhtinen, et al., NIM A 545 (2005) 63–87.
[11] P. Lecomte, D. Luckey, F. Nessi-Tedaldi, F. Pauss, NIM A 564 (2006) 164–168.
[12] Ren-Yan Zhu, J. Phys.: Conf. Ser. 928 (2017) 012015.
[13] E. Auffray, A. Fedorov, et al., NIM A 856 (2017) 7–10.
[14] Fan Yang, et al., J. Phys.: Conf. Ser. 928 (01) (2017) 2029.
[15] LHCb Collaboration, LHCb Calorimeters TDR, CERN/LHCC/2000-0036 (2000).
[16] G. Tamulaitis, et al., NIM A 870 (2017) 25–29.
[17] M. Korjik, et al., NIM A 871 (2017) 42–46.
[18] Patent RF2646407, 02.06.2017 (in Russian).
[19] M.T. Lucchini, et al., NIM A 816 (2016) 176–183.
[20] The FLUKA Code: Developments and Challenges for High Energy and Medical Applications, T.T. Böhlen, F. Cerutti, M.P.W. Chin, A. Fass, A. Ferrari, P.G. Ortega, A. Mairani, P.R. Sala, G. Smirnov, V. Vlachoudis, Nucl. Data Sheets 120 (2014) 211–214.